

naka and K. Yoshino, *J. Chem. Phys.* **57**, 2964 (1972).

²T. R. Dyke, G. R. Tomasevich, W. Klemperer, and W. E. Falconer, *J. Chem. Phys.* **57**, 2277 (1972); S. E. Novick, P. Davies, S. J. Harris, and W. Klemperer, *J. Chem. Phys.* **59**, 2273 (1973).

³D. Kleppner, in *Atomic Physics 2*, edited by G. K. Woodgate and P. G. H. Sandars (Plenum, New York, 1971), p. 177.

⁴C. C. Bouchiat, M. A. Bouchiat, and L. C. Pottier,

Phys. Rev. **181**, 144 (1969); C. C. Bouchiat and M. A. Bouchiat, *Phys. Rev. A* **2**, 1274 (1970); M. A. Bouchiat, J. Brossel, and L. C. Pottier, *J. Chem. Phys.* **56**, 3703 (1972).

⁵R. M. Herman, *Phys. Rev.* **136**, A1576 (1964).

⁶M. A. Bouchiat and L. C. Pottier, *J. Phys. (Paris)* **33**, 213 (1972).

⁷F. Y. Chu, thesis, Massachusetts Institute of Technology, 1972 (unpublished).

Investigation of the Production of Noncharacteristic X Rays during Ar-Si Collisions at 270 keV

J. A. Cairns, A. D. Marwick, J. Macek,* and J. S. Briggs

Atomic Energy Research Establishment, Harwell, Didcot, Berkshire, United Kingdom

(Received 26 November 1973)

This study elucidates the role played by implanted argon in the production of Ar *L*, non-characteristic, and Si *K* x rays during 270-keV argon bombardment of silicon carbide.

Recent observations¹⁻⁶ of noncharacteristic x rays produced during bombardment of solids by energetic heavy ions have been interpreted¹ as being due to inner-shell transitions during the lifetime of the pseudomolecule formed during an atomic collision. In this paper we present a study of the phenomenon, in which the relationship between characteristic and noncharacteristic x rays is clarified. The system studied is Ar + Si, since three groups of x rays arise, which can be easily resolved; namely Ar *L* (~220 eV), noncharacteristic (whose distribution appears to peak at 1 keV because of the strong attenuation exhibited by the detector window for the lower energy components), and Si *K* (~1800 eV).

The Fano-Lichten model⁷⁻⁹ of heavy-ion x-ray production predicts that no Si *K* x rays are produced in a single collision between argon and silicon atoms, because the 1s electrons of silicon would have to be promoted to the argon 2*p*, which is already full. The fact that Si *K* x rays are generated was explained by Macek, Cairns, and Briggs¹⁰ as arising from a double scattering in which an argon 2*p* vacancy created in a prior collision is carried into a subsequent Ar-Si collision, thereby permitting Si *K*-electron promotion. The production of noncharacteristic x rays is thought to be an alternative process during the same collision. It thus becomes apparent that all three x-ray yields, viz. Ar *L*, noncharacteristic, and Si *K*, are interrelated.

The x-ray yields measured in our experiment are shown in Fig. 1. Targets of silicon and sili-

con carbide were bombarded with 270-keV Ar⁺⁺ ions. The x rays emitted were detected with an end-window proportional counter¹¹ and single-channel-analyzers were used to obtain the yields of the three x rays. The yields are not corrected for absorption in the counter window. However, the rate of buildup of the x-ray yields shown in Fig. 1, expressed as a fraction of their initial yields extrapolated to zero dose, can be correctly determined from the data, as can differences in intensity between silicon and silicon-carbide targets.

In their original study of this system, Saris, van der Weg, and Tawara¹ observed that the non-

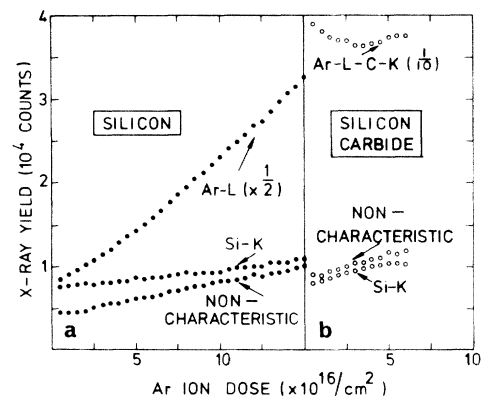


FIG. 1. The yields of Ar *L* (220 eV), noncharacteristic (band), and Si *K* (1739 eV) x rays under 270-keV Ar⁺⁺ bombardment as argon dose is increased. The yields of all three x rays are higher in the case of SiC targets.

characteristic x-ray yield increased with argon projectile dose. This led them to postulate that these x rays were due to Ar-Ar collisions. However, we see from Fig. 1(a) that not only does the noncharacteristic x-ray yield increase with dose, but so also does the Ar *L* yield and the Si *K* yield. We may explain this within the double-collision model by demonstrating that the accumulation of argon within the target, which tends to enhance the probability of Ar *2p* vacancy production, will in turn increase the likelihood of generating both noncharacteristic x rays and Si *K* x rays. Therefore it would appear more likely that the noncharacteristic x rays arise from Ar-Si collisions, rather than from Ar-Ar collisions. At larger argon doses than we have reached, Ar-Ar noncharacteristic x rays are expected to appear, as Bissinger and Feldman⁶ have confirmed.

We may note at this point that an alternative method of producing Si *K* x rays may be thought to arise from the interaction of an argon projectile and a silicon target atom, resulting in the latter recoiling with sufficient energy to produce a Si *K* x ray on a subsequent Si-Si collision.¹² Since the recoiling silicon could quickly obtain a *2p* vacancy, the production of noncharacteristic x rays can arise during the Si-Si collisions. The upper energy limit for such x rays according to the current model¹ would be 850 eV (Ni *L*) and thus most would be absorbed in the window of the counter. No buildup of silicon recoil noncharacteristic x rays is expected, but a small fraction of the noncharacteristic x rays observed may be due to this process. In addition we shall see that our results indicate that a fraction of the observed Si *K* yield is due to silicon recoils.

Again referring to Fig. 1(a), we note the following:

(i) All the x-ray yields build up approximately linearly. This indicates that the yields depend linearly on argon concentration. In particular, the linear increase in the noncharacteristic x rays favors the interpretation that these arise from Ar-Si collisions, rather than from Ar-Ar collisions, which would cause them to build up quadratically.

(ii) The rate of buildup of Ar *L* intensity, relative to its initial value, is nearly twice the rate of buildup of the noncharacteristic x ray. This is because the Ar *L* yield comes from vacancies in both projectile and implanted Ar atoms, but only the former—half the total—can subsequently induce a noncharacteristic x ray. (For example, the cross section for *2p* vacancy production

in an Ar-Ar collision is 100 times larger than that for production of an argon recoil with energy greater than one quarter of the incident ion energy.) The anomalous behavior of the Si *K* yield, which increases at only a quarter of the rate of the noncharacteristic x rays, is probably a consequence of a contribution from Si+Si recoil collisions, as pointed out by Taulbjerg, Fastrup, and Laegsgaard.¹² This contribution should be rather insensitive to Ar dose. If, in qualitative agreement with the measurement of Taulbjerg, Fastrup, and Laegsgaard, one allows 75% of the initial Si *K* yield to be due to recoils, then the discrepancy in buildup rates of Si *K* and noncharacteristic x rays can be accounted for.

As a further demonstration of the buildup effect, we may now examine a complementary system. Thus Fig. 1(b) shows the effect of increasing argon dose during 270-keV argon bombardment of silicon carbide. In this system the production of argon *2p* vacancies in Ar+C collisions should considerably increase the proportion of Ar projectiles having *2p* vacancies. The resulting increase in Ar *L* x-ray production is demonstrated in the high-resolution data described below (Fig. 2). A further consequence of increased Ar *2p* vacancy production is that the yields of both noncharacteristic and Si *K* x rays are higher in SiC than in Si. Both x rays also exhibit an increase in yield with increasing argon dose.

We have determined that the increased yield of noncharacteristic x rays observed with an SiC target is not due to recoil C+C molecular x rays,⁵ by measuring the yield of noncharacteristic x rays in the bombardment of SiC by carbon

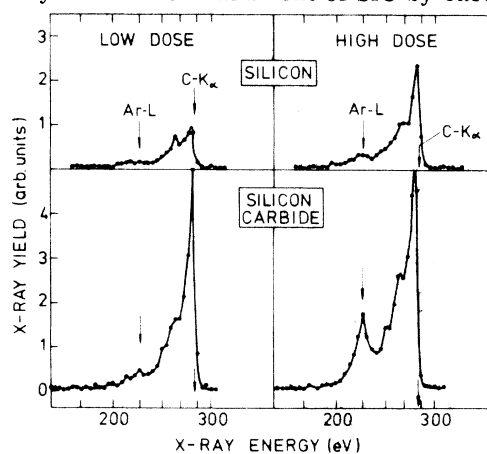


FIG. 2. The spectrum of the low-energy x rays emitted during Ar bombardment of Si and SiC. Note the presence of Ar *L* "normal" line (220 eV) and in the case of SiC, the C *K* (277 eV). Low dose, about 10^{17} ions cm^{-2} ; high dose, about 5×10^{17} ions cm^{-2} .

ions at different energies. By integration of the resulting yield-energy curve with the Ar-C elastic scattering cross section,¹³ the recoil-molecular cross section and hence yield was calculated, and found to be negligible.

One interesting feature of the SiC system shown in Fig. 1(b) is that the "Ar *L*" yield is much higher than for Ar-Si collisions at the same energy, and shows a quite different dose dependence. We may explain this by the observation that during Ar-SiC collisions, many more C *K* than Ar *L* x rays are produced (this will be verified by x-ray spectral measurements reported below); hence the apparent absence of Ar *L* buildup. [Note that Ar *L* (220 eV) and C *K* (277 eV) x rays are too similar in energy to be resolved by a proportional counter.]

Thus, this system proves that the important condition for the production of both noncharacteristic x rays and Si *K* x rays is the prior production of Ar *2p* vacancies. Note how the noncharacteristic x-ray yield is higher than in the Ar-Si system right from the start, before there could be any substantial buildup of argon. Also, while the Si *K* yield is initially similar to that in Ar-Si, its rate of buildup is now the same as that of the noncharacteristic x rays. This can be explained by the lower Si *K* yield expected from Si recoils in SiC, because of the presence of carbon, which attenuates the collision cascades. Thus almost the entire Si *K* yield seems to be due to the enhanced Ar *2p* vacancy production and the buildup rates of both noncharacteristic and Si *K* yields are controlled by Ar *2p* vacancy production.

An additional insight into these processes is obtained by examining the degree of excitation of the argon projectile during the collisions. This was done by using a grating spectrometer,¹⁴ incorporating a new low-noise proportional counter.¹⁵ The resolution of the spectrometer was 3.5 Å. Figure 2 shows the Ar *L* spectra obtained from Ar-Si bombardment at 270 keV, before and after argon dose buildup, and also shows those obtained from Ar-SiC collisions under similar conditions. In examining spectra such as Fig. 2, one must keep in mind that the intensity above the C *K* edge (284 eV) is strongly attenuated by absorption in the counter window. Note how the Ar-SiC spectra are dominated by C *K* x rays (277 eV) as mentioned above, while the Ar *L* (220 eV), although building up, is relatively small. Note also the increased yield of Ar *L* in the case of SiC. The C *K* yield does not, of

course, build up with argon dose. In addition to the normal Ar *L* line at 220 eV, both sets of spectra contain an additional satellite line at 250 eV. This line most likely arises from an argon ion with one *2p* vacancy and several outer-shell vacancies.

Furthermore, the Ar-Si spectra show another satellite at 270 eV. This line may also arise from an argon ion with one *2p* vacancy and several outer-shell vacancies, or from an argon ion with two *2p* vacancies. One can see from the figure that it builds up more quickly than the 250-eV line. Naturally this effect is obscured in the Ar-SiC case by the presence of the C *K* line.

In summary, these observations are generally consistent with the idea originally postulated by Saris and co-workers as to the origin of the non-characteristic x rays which arise during argon-ion bombardment of silicon, although they point to Ar-Si collisions as being the dominant mechanism. The purpose of *this* work has been to establish more precisely the role played by the projectile in these processes, and to show how this in turn is related to the yields of characteristic x rays from both the target and the projectile.

Our thanks are due to Peter Chandler for his help in taking data.

*Permanent address: Behlen Laboratory of Physics, University of Nebraska, Lincoln, Neb. 68508.

¹F. W. Saris, W. F. van der Weg, and H. Tawara, *Phys. Rev. Lett.* **28**, 717 (1972).

²F. W. Saris, I. V. Mitchell, D. C. Santry, J. A. Davies, and R. Laubert, in *Proceedings of the International Conference on Inner Shell Ionization Phenomena and Future Applications, Atlanta, Georgia, 1972*, edited by R. W. Fink, J. T. Manson, I. M. Palms, and R. V. Rao, CONF-720 404 (U.S. Atomic Energy Commission, Oak Ridge, Tenn., 1973).

³P. H. Mokler, H. J. Stein, and P. Armbruster, *Phys. Rev. Lett.* **29**, 827 (1972).

⁴J. R. Macdonald and M. D. Brown, *Phys. Rev. Lett.* **29**, 4 (1972).

⁵J. R. Macdonald, M. D. Brown, and T. Chiao, *Phys. Rev. Lett.* **30**, 471 (1973).

⁶G. Bissinger and L. Feldman, *Phys. Rev. A* **8**, 1624 (1973).

⁷U. Fano and W. Lichten, *Phys. Rev. Lett.* **14**, 627 (1965).

⁸W. Lichten, *Phys. Rev.* **164**, 131 (1967).

⁹M. Barat and W. Lichten, *Phys. Rev. A* **6**, 211 (1972).

¹⁰J. Macek, J. A. Cairns, and J. S. Briggs, *Phys. Rev. Lett.* **28**, 1298 (1972).

¹¹J. A. Cairns, C. L. Desborough, and D. F. Holloway, *Nucl. Instrum. Methods* **88**, 239 (1970).

¹²K. Taulbjerg, B. Fastrup, and E. Laegsgaard, Phys. Rev. A **8**, 1814 (1973).

¹³K. Taulbjerg and P. Sigmund, Phys. Rev. A **5**, 1285 (1972).

¹⁴M. Steadman, J. A. Cairns, and A. D. Marwick, to be published.

¹⁵J. A. Cairns, D. F. Holloway, and G. F. Snelling, Nucl. Instrum. Methods **111**, 419 (1973).

Observation of the High-Resolution Mössbauer Resonance in ⁷³Ge

R. S. Raghavan and Loren Pfeiffer

Bell Laboratories, Murray Hill, New Jersey 07974

(Received 14 January 1974)

The high-resolution Mössbauer effect of the 13.3-keV transition ($\tau = 4.3 \mu\text{sec}$) in ⁷³Ge has been observed in transmission experiments at room temperature. The recoilless γ -ray source was carrier-free ⁷³As diffused into a single crystal of elemental germanium; the absorber was a thin single-crystal layer of enriched ⁷³Ge epitaxially grown on a silicon substrate. The resonance absorption line, recorded with an electromechanical velocity spectrometer, has a corrected depth of $\sim 2.0\%$, and a (full width at half-maximum) linewidth 2Γ of $47(7) \mu\text{m/sec}$, which is ~ 7 times the natural linewidth. Despite the broadening this is the narrowest Mössbauer resonance observed so far at room temperature.

Since the early days of the Mössbauer effect, the 13.3-keV transition in ⁷³Ge has been one of the most attractive candidates for high-resolution experiments, because of the extreme sharpness of the resonance ($E/\Gamma_0 \approx 10^{14}$), the conveniently long lifetime of the parent nuclide ⁷³As ($T_{1/2} = 80$ days), and the low energy of the γ ray which assures a high probability for recoilless transitions even at room temperature. Observation of this resonance, with a potential 28-fold improvement in E/Γ_0 over the well-known 14.4-keV transition in ⁵⁷Fe, would constitute a major advance in the search for a high-resolution tool of this type for use in solid-state and general physics experiments. In this Letter we report the discovery of the resonance. At this preliminary stage the width of the absorption line is about 7 times the natural linewidth; despite this broadening, however, it is already the narrowest Mössbauer line observed so far at room temperature.

The nuclear spectroscopic information on the electron-capture decay of ⁷³As \rightarrow ⁷³Ge was not clarified until recently, when several groups were able to do so using high-resolution Si(Li) detectors.¹ The currently accepted level parameters are summarized in the decay-scheme in the inset of Fig. 1. The main difficulties in the observation of the 13.3-keV resonance in ⁷³Ge arise from (a) the high total internal conversion coefficient of the γ ray ($\alpha_T = 1100$), (b) the close proximity of its energy to the *K*-absorption edge of Ge (11.1 keV), and (c) the low natural abun-

dance of ⁷³Ge (7.76%). Because of (a) and (b) the resonance cross section is *smaller* than the non-resonant electronic absorption cross section in Ge at 13.3 keV ($\sigma_{\text{res}}/\sigma_{\text{el}} = 0.5$), a situation unusual in a Mössbauer experiment. In practice this forces the choice of either using a thin absorber and thus reducing the potential resonance effect, or having to contend with a severe reduction in the spectral quality of the detected 13.3-keV

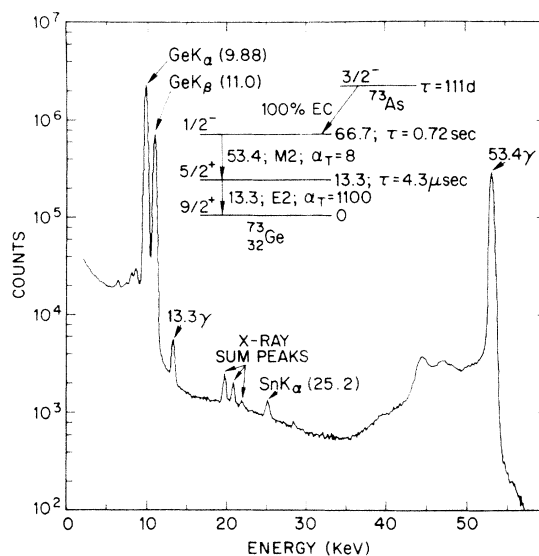


FIG. 1. Energy spectrum of ⁷³As source in the Mössbauer geometry (see text) with 10-mg/cm² ⁷³Ge absorber, recorded with a Si(Li) detector. The energies of the lines are in keV. Inset, decay scheme of ⁷³As \rightarrow ⁷³Ge; τ is the mean life.